Total Synthesis of Tetrodotoxin and 9-*epi*Tetrodotoxin

Xiangbing Qi (qixiangbing@nibs.ac.cn)
National Institute of Biological Sciences, Beijing https://orcid.org/0000-0002-7139-5164
Pei-hao Chen
Peking University
Jing Wang
School of Life Sciences, Tsinghua University https://orcid.org/0000-0003-3378-2099
Yan Wang
National Institute of Biological Sciences, Beijing
Yuze Sun
National Institute of Biological Sciences, Beijing
Songlin Bai
National Institute of Biological Sciences,Beijing
Qingcui Wu
National Institute of Biological Sciences, Beijing
Shuangfeng Zhang
National Institute of Biological Sciences, Beijing
Xinyu Cheng
National Institute of Biological Sciences, Beijing
Peng Cao
National Institute of Biological Sciences, Beijing https://orcid.org/0000-0001-7739-6857

Article

Keywords:

Posted Date: January 24th, 2023

DOI: https://doi.org/10.21203/rs.3.rs-2459518/v1

Additional Declarations: Yes there is potential Competing Interest. The authors (Peihao Chen, Jing Wang, Yan Wang, Yuze Sun, Qingcui Wu, Xiangbing Qi) declare a patent application based on this study (WIPO

Application No. PCT/CN2022/111861).

Version of Record: A version of this preprint was published at Nature Communications on January 23rd, 2024. See the published version at https://doi.org/10.1038/s41467-024-45037-0.

Abstract

Tetrodotoxin and congeners are specific voltage-gated sodium channel blockers that exhibit remarkable anesthetic and analgesic effects. Here, we present a scalable asymmetric synthesis of TTX and 9-*epi*TTX from the abundant chemical feedstock furfuryl alcohol. The optically pure cyclohexane skeleton was assembled via a stereoselective Diels-Alder reaction. The dense heteroatom substituents were established sequentially by a series of functional group interconversions on highly oxygenated cyclohexane frameworks, including a chemoselective cyclic anhydride opening, and a decarboxylative hydroxylation. An innovative SmI_2-mediated concurrent fragmentation, an oxo-bridge ring opening and ester reduction followed by an Upjohn dihydroxylation delivered the highly oxidized skeleton. Ruthenium-catalyzed oxidative alkyne cleavage and formation of the hemiaminal and orthoester under acidic conditions enabled the rapid assembly of TTX, anhydro-TTX, 9-*epi*TTX, and 9-*epi* lactone-TTX.

Full text

Tetrodotoxin (TTX, **1**), is one of the most potent neurotoxins with a complex structure, and analgesic effects. After the first isolation of TTX in 1909,[1] the structure of this highly polar zwitterion was solved by Woodward,[2,3] Tsuda,[4] Goto,[5] and Mosher[6] simultaneously in 1964 using degradative methods and NMR spectroscopy. TTX's unique structure comprises a densely heteroatom-substituted, stereochemically complex framework that has a rigid dioxa-adamantane cage with an ortho acid, a cyclic guanidinium hemiaminal moiety, and nine contiguous stereogenic centers, including one bridgehead nitrogen-containing quaternary center. There are three compounds in equilibrium—ortho ester, 4,9-anhydro, and lactone, that are known to interconvert under acidic conditions.[7,8] Recently, the TTX analogue 9-*epi*Tetrodotoxin (**1a, Figure 1**) was isolated as an equilibrium mixture of the hemilactal and 10,8-lactone forms.[9] TTX is neurotoxic and exhibits prominent anesthetic and analgesic properties in animal models. The mode of action of this bipolar molecule is defined by its disruption of voltage-gated sodium ion channels (Na_v), which was originally suggested in the early 1960s,[10,11] and was recently confirmed by crystallographic studies.[12,13] Extensive pharmacological investigations, including clinical trials,[14] have demonstrated the immense promise of TTX in pain treatment and detoxification from heroin addiction; accordingly, a reliable source of TTX is of practical significance.

The remarkably polar functionality, stereochemically complex architecture, and fascinating biological activity, have made this compound an attractive synthetic target. To date, numerous efforts have been made towards the total synthesis of TTX, with the first synthesis by Kishi in 1972.[15,16] Subsequently, asymmetric syntheses have been achieved by Isobe,[8,17] Du Bois,[18] Sato,[19-21] Fukuyama,[22] Yokoshima,[23] and Marin.[24] More recently, Trauner described an elegant and concise asymmetric synthesis of TTX based on a glucose derivative.[25] In addition to these syntheses, TTX has

also been a model compound for demonstrating creative synthetic strategies, in assembling this type of highly oxygenated guanidinium alkaloids efficiently (Keana,[26-28] Burgey,[29] Alonso,[30-33] Taber,[34]

Shinada,[35] Ciufolini,[36,37] Hudlicky,[38] Nishikawa[39-42] and Johnson[43,44]).

Precise functional group manipulations on heavily heteroatom-substituted, stereochemically complex frameworks have proven challenging, as evidenced by the total synthesis of highly oxidized natural products,[45-53] and as exemplified by the synthetic studies of TTX by Isobe,[8] Du Bios,[18] Sato,[19,20] Yokoshima,[23] and Trauner[25](**Figure 1**) using highly oxygenated natural starting materials such as, *D*-glucose (**2**), myo-inositol (**3**), *D*-mannoside (**4**), or *D*-isoascorbic acid (**5**). Although the preexisting oxygen functionality in these naturally occurring materials provides the functionality basis of TTX, efficient and precise interconversion of these similar functionalities on the densely heteroatom-substituted skeleton in a chemo and stereoselective manner is arduous. We envisioned that if the highly oxygenated framework could be assembled rapidly in the early stage in a stereo-controllable fashion and followed by sequential chemo and stereoselective functional group manipulations might provide a practical solution to a concise synthesis of TTX and its congeners (**Figure 1**). Here, we describe a distinct synthetic strategy that streamlines the incorporation of the dense heteroatom-substituted architecture and is amenable to a scalable synthesis of 9-*epi*TTX and TTX (>15 mg, which is the largest scale known in literature).

Retrosynthetic analysis (**Figure 1**) reveals that the hemiaminal and orthoester moieties of the complex dioxa-adamantane architecture can be obtained in one step from intermediate **6**, in which both the ester and guanidinium groups are built upon the bridgehead oxygen functionality of framework **7** via a series of well-planned events: SmI_2-mediated reductive oxo-bridge ring opening, Dess-Martin oxidation, chloroepoxidation,[20,54,55] stereoselective epoxide opening, and ruthenium-catalyzed oxidative alkyne cleavage. The anhydride motif of **7** is initially transformed into chemically differentiated mono-acid and mono-ester by regioselective methanolysis, which lays the foundation for subsequent radical decarboxylative hydroxylation and hemiaminal synthesis from the redox manipulation of the ester. To access the highly oxygenated chiral framework **7**, a stereoselective strategy is proposed from a chiral auxiliary assisted Diels-Alder reaction of the easily accessible maleic anhydride **8** and furfuryl alcohol **9**.

The synthesis of TTX (**1**) was initiated with the stereoselective construction of the oxygen-substituted cyclohexane skeleton (**Figure 2**). The first oxygen functionality was derived from furfuryl alcohol **9** directly. Esterification of furfuryl alcohol **9** with chiral auxiliary (-)-(1*S*)-camphanic acid afforded ester **10**. To achieve the enantiomerically pure 7-oxabicyclo[2.2.1]hept-2-ene derivative **11**,[56] we developed a reliable stereoselective Diels-Alder protocol by heating **10** with maleic anhydride in the presence of isopropyl ether as the solvent (see **Figure 3a and Table S1**). Initially, the original pro-

tocol by Vogel[56] under neat conditions was attempted, but only a 5:4 mixture of two inseparable *exo* adducts **11** and **11a** was observed (by ^{1}H-NMR analysis of the reaction mixture). Investigation of reaction conditions including the effects of molar ratio of reactants, Lewis acids, reaction time, and the temperature was unfruitful in terms of either yield or diastereoselectivity.

Consequently, a survey of solvents was conducted and the use of isopropyl ether was found to be the crucial factor for the successful generation of optically pure diastereomer **11** as a single detectable *exo*

cycloadduct **(ratio of 11**: **11a >20:1)**. The high *exo*-selectivity observed in the current cycloaddition is presumably resulted from the retro-Diels–Alder fragmentation of unstable *endo* cycloadduct.[57] However, whether the chiral auxiliary (-)-(1*S*)-camphanic acid plays a stereoselective control for Diels–Alder cycloaddition or promotes the crystallization-based enrichment is still a puzzle since no other diastereomers were detected during the whole process, which is inconsistent with the observation by Vogel[56]. This stereoselective cycloaddition established the second oxygen functionality and could be scaled up to 100 grams without erosion of yield or stereoselectivity. Quinine-mediated regioselective methanolysis[58] of anhydride **11** resulted in the methyl ester and acid **12**. Subsequently, a stereospecific Upjohn *exo*-dihydroxylation[59] of the olefin established the third and the fourth oxygen functionalities (with simultaneous 1,2-diol protection) and produced the mono-acid **13**, whose structure was confirmed by X-ray crystallographic analysis of the single crystal (CCDC#: 2184304).

Decarboxylative hydroxylation was carried out to introduce the fifth oxygen functionality at the C5 position. Initially, high-valent metal reagents were examined as oxidants but were inadequate owing to substrate decomposition. Mild radical conditions, including Barton or organophotoredox-promoted decarboxylation in the presence of a radical initiator and oxygen under UV irradiation,[60-62] were also unsuccessful (see **Figure 3b**). After considerable experimentation, a Ru-catalyzed photore-

dox decarboxylative hydroxylation[63] of the *N*-hydroxyphthalimide (NHPI) ester of **13** produced **14** as a single detectable diastereomer in 66% yield, albeit with an inverted configuration at C5 relative to TTX. Previous syntheses[8,18] revealed that steric hindrance at the C5 position is troublesome for the following functional group manipulations. Therefore, we utilized a late-stage configurational inversion strategy to simplify the stereoselective oxygen functionality installation sequence. Notably, this photoredox decarboxylative hydroxylation could also be scaled up by employing circulating flow photochemistry without compromising the yields or diastereoselectivity (**entry 4**, **Figure 3b**). To interpret the diastereoselectivity and analyze the steric effect of this radical addition, we performed the density functional theory (DFT) calculations. The DFT calculations support a clear radical addition preference for the experimentally observed stereoisomer at C5 that stems from the radical addition from the convex face of the oxo-bridge ring. ($\Delta\Delta G$=3.4 kcal/mol and predicted dr > 99:1, details of computation results are shown in the supplementary information.)

With compound **14** in hand, we investigated the functional group interconversions of this oxo-bridge ring system and developed a reaction sequence to build the oxygen functionalities at the C8a, C6, and C11 positions. The auxiliary (-)-camphanic acid was first removed by transesterification with methanol, providing the primary alcohol, which was then subjected to an Appel reaction giving the alkyl iodide **15**. The chiral auxiliary could be recycled as methyl camphanate. A variety of reductive conditions applied to the alkyl iodide **15** failed to produce the desired oxo-bridge ring-opening product. After intensive exploration of the reductive conditions, we developed a successful reaction sequence (**Figure 3c**): the initial SmI_2 mediated single electron transfer homolytically cleaved the carbon-iodide bond and generated a primary carbon radical, which could be further reduced by Sm(II) to a carbanion[64,65] to drive the bridged

C-O bond cleavage. The primary alcohol was generated from concurrent methyl ester reduction by SmI_2, while the N-O bond of TEMPO remained unaffected due to steric hindrance. In the presence of hexamethylphosphoramide (HMPA), only intermediate **16a** was obtained without reduction of the methyl ester to diol **16** (**entry 1**, **Figure 3c**). Activation of SmI_2 with H_2O and Et_3N in a 1:2:2 ratio created a stronger reductant,[66] which allowed for the reduction of the methyl ester (**entry 2**) in a 77% yield as determined by ^1H NMR. Increasing amounts of H_2O and Et_3N or replacing Et_3N with pyrrolidine resulted in complex product mixtures (**entries 3** and **4**). The procedure could also be modified to a two-step protocol involving fewer equivalents of SmI_2 to afford **16a**, followed by a $LiAlH_4$ reduction to give **16** in 58% yield on a decagram scale (**entry 5**). The relative configuration of **16** was verified by X-ray crystallography of the single crystal (CCDC#: 2182018).

The construction of azidoaldehyde **20** started with selective protection of the primary alcohol in **16** using the sterically hindered TBDPSCl. The N-O bond of TEMPO in the resulting alkene was reductively cleaved with Zn powder giving the allylic alcohol **17**. The incorrect configuration of C5-OH was then inverted by a chemoselective Mitsunobu reaction of C5 allylic alcohol in the presence of free C8a secondary alcohol with 2-methoxyacetic acid **27**, delivering the fifth oxygen functionality in **18** in excellent yield. Other acids such as acetic acid or benzyloxyacetic acid afforded products in low yields. The sixth and seventh oxygen functionalities were established via a diastereoselective Upjohn dihydroxylation followed by protection as the acetonide, whose relative configuration was confirmed by X-ray crystallography of the derivative **21** (CCDC#: 2184298) (See the supplementary information). The secondary alcohol underwent Dess-Martin oxidation to afford the ketone **19** in excellent yield. An intramolecular Mannich reaction between the *α* position of methoxyacetic acid and the ketone **19** derived imine was unfeasible. The intermolecular nucleophilic addition of a variety of nucleophiles also exclusively produced a diastereomer with the wrong configuration at C8a (See **Scheme S2**). Although Darzens reaction of **19** with *α*-haloester smoothly generated an *α*, *β*-epoxy ester (glycidic ester), the stereoselective and regioselective epoxide opening strategy proved unfruitful in the presence of different types of nitrogen-based nucleophiles (**Scheme S2**). The nucleophilic addition of Sato's dichloromethyllithium ($LiCHCl_2$) to the ketone **19** was successfully afforded the spiro *α*-chloroepoxide as a single diastereomer[20,54] and concurrently removed the ester group at C5-OH, which was protected with a *p*-methoxybenzyl group (PMB) in one pot. Regioselective epoxide opening of the resulting chloroepoxide with NaN_3 proceeded smoothly to afford the *α*-azido aldehyde **20** on a gram-scale, with the correct configuration of the C8a quaternary stereogenic center.

With the construction of the highly oxygen-substituted carbocyclic core **20** accomplished, we began to address the synthetic challenge of constructing the complex dioxa-adamantane core and the guanidinium hemiaminal moieties. The *α*-azido aldehyde **20** was subjected to a 1,2-addition with lithium acetylide (**Table S2**), followed by the removal of the TBDPS group to produce two diastereomers (**22**/**22a**=1:15) that could undergo divergent synthesis to both TTX and *9-epi*TTX. Presumably owing to the steric hindrance introduced by the bulky TBDPS and PMB groups, the lithium acetylide preferentially attacked from the less sterically hindered *si* face and generated the undesired diastereomer **22a** (**Figure**

3d). Extensive exploration of the reaction conditions revealed that the stereochemistry of C9 of **22a** could be inverted in a 2:1 ratio (**22**/**22a**=2:1) via sequential MnO_2-mediated chemoselective oxidation followed by $NaBH_4$ reduction (**Table S3**). IBX oxidation of the primary alcohol **22** provided the corresponding bridged hemiacetal, which was converted to the acetal **23** with trimethylorthoacetate. The structure and the stereochemistry of **23** were confirmed by single-crystal X-ray crystallography (CCDC#: 2184305). Distinct from previous syntheses that heavily focused on the lactone formation between C5-OH and the C10-COOH as the advanced intermediate, our strategy pinpointed the issue of conformational control for precise functional group manipulations on the stereochemically complex framework. Decreasing the conformational flexibility by the bridged tetrahydrofuran acetal ring formed between C9 and C4 is critical to the efficiency of the following transformations including alkyne oxidative cleavage, guanidine installation, and one-step cyclic guanidinium hemiaminal and orthoester formation, thus demonstrating a unique and concise strategy for the final stage of TTX synthesis.

Oxidative cleavage of alkyne **23** with $RuCl_3$/$NaIO_4$ followed by esterification afforded methyl carboxylate **24**. Simultaneous PMB deprotection and azido reduction by hydrogenation efficiently delivered the tertiary amine, which was guanidinylated[67] *in situ* with bis-Boc protected isothiourea **26**, leading to the penultimate intermediate **25**. To our delight, treatment of this unprecedented compound **25** with trifluoroacetic acid at 60 °C afforded a global deprotection and successfully installed both the hemiaminal and the orthoester of TTX, leading to the final product TTX (**1**) and 4,9-anhydroTTX (**1b**) in a 1:1 mixture. The use of 2% TFA-*d* in deuterium oxide further converted this mixture to a 4:1 ratio favoring TTX (see supplementary information).[8] A similar synthetic process was used to convert the diastereomer **22a** to the final 9-*epi*TTX (**1a**) and its 10,8-lactone form (**1c**) in 5 steps (14% overall yields). The spectroscopic data (^{1}H NMR, ^{13}C NMR, HRMS) of synthetic TTX and 9-*epi*TTX were identical to those of the authentic reference samples[7,8].

TTX in most biomedical studies is a mixture in equilibrium with the ortho ester, the lactone form, and 4,9-anhydroTTX. [8,11] To investigate the biological activities of a pure TTX , we synthesized and purified a single form of TTX (**S**) from the methyl carboxylate **24** (**Figure 4a**) according to Fukuyama's strategy.[22] A commercial sample named TTX (**C**) (the ratio of TTX to 4,9-anhydroTTX was 3:1 as analyzed by ^{1}H NMR, **Figure S1**) was utilized for comparison. In mice, primary hippocampal neurons cultured for 14 days displayed a mature sodium current property (**Figure 4b**). Both samples at 1μM concentration were sufficient to block sodium currents in cultured hippocampal neurons (**Figure 4c**). Next, we detected the Na_v blocking effects of these two TTX samples across a range of concentrations (10 nM, 50 nM, 100 nM). Compared to TTX (**C**), our synthetic pure TTX (**S**) showed a stronger effect in decreasing the sodium current amplitude in wild-type div (days *in vitro*) 14 hippocampal neurons (**Figure 4d**).

In summary, we have achieved the first asymmetric synthesis of 9-*epi*TTX (**1a**) (22 steps) and one of the shortest syntheses of TTX (**1**) (24 steps, following the Rules for Calculating Step Counts[68,69]) from the easily accessible furfuryl alcohol. The hundred-gram-scale asymmetric preparation of cyclohexane (+)-**12** showcases the power of the stereoselective Diels-Alder reaction in the scale-up synthesis of a carbocyclic

ring with a dense array of functionalities.[70] The precise introduction of the oxygen functionality at the C-5 position via photochemical decarboxylative hydroxylation highlights the advance of free radical transformation performed on a sterically demanding carbocyclic skeleton. The SmI_2-mediated sequential reactions of reductive fragmentation, oxo-bridge ring opening, and ester reduction, followed by diastereoselective Upjohn dihydroxylation enable a gram-scale synthesis of highly oxidized intermediate (+)-**19**. The bridged tetrahydrofuran acetal setting simplifies the endgame and facilitates the rapid formation of the cyclic guanidinium hemiaminal and orthoester in one pot. Notably, the present synthesis served as a testbed for precise functional group manipulations on the densely functionalized and stereochemically complex frameworks and should be readily applicable to the synthesis of other heavily oxygenated polycyclic natural products. The concise synthetic strategy is suitable for the production of TTX congeners or derivatives that support further pharmacology investigations and should be amenable to large-scale synthesis of TTX for analgesic drug development, particularly for non-opioid cancer pain treatment.

References

1. Tahara, Y. & Hirata, Y. Studies on the puffer fish toxin. J. Pharm.Soc.Jpn. **29**, 587–625 (1909).
2. Woodward, R. B. The structure of tetrodotoxin. Pure and Applied Chemistry **9**, 49–74 (1964).
3. Woodward, R. B. & Gougoutas, J. Z. The Structure of Tetrodotoxin. J. Am. Chem. Soc. **86**, 5030–5030 (1964).
4. Tsuda, K. *et al.* On the constitution and configuration of anhydrotetrodotoxin. Chem. Pharm. Bull. **12**, 634–642 (1964).
5. Goto, T., Kishi, Y., Takahashi, S. & Hirata, Y. Tetrodotoxin. Tetrahedron **21**, 2059–2088 (1965).
6. Mosher, H. S., Fuhrman, F. A., Buchwald, H. D. & Fischer, H. G. Tarichatoxin—Tetrodotoxin: a potent neurotoxin. Science **144**, 1100–1110 (1964).
7. Yasumoto, T., Yotsu, M., Murata, M. & Naoki, H. New tetrodotoxin analogs from the newt Cynops ensicauda. J. Am. Chem. Soc. **110**, 2344–2345 (1988).
8. Ohyabu, N., Nishikawa, T. & Isobe, M. First Asymmetric Total Synthesis of Tetrodotoxin. J. Am. Chem. Soc. **125**, 8798–8805 (2003).
9. Yaegashi, Y. *et al.* Isolation and Biological Activity of 9-*epi*Tetrodotoxin and Isolation of Tb-242B, Possible Biosynthetic Shunt Products of Tetrodotoxin from Pufferfish. J. Nat. Prod. **85**, 2199–2206 (2022).
10. Narahashi, T., Moore, J. W. & Scott, W. R. Tetrodotoxin blockage of sodium conductance increase in lobster giant axons. J. Gen. Physiol. **47**, 965–974 (1964).
11. Makarova, M., Rycek, L., Hajicek, J., Baidilov, D. & Hudlicky, T. Tetrodotoxin: History, Biology, and Synthesis. Angew. Chem., Int. Ed. **58**, 18338–18387 (2019).
12. Shen, H. *et al.* Structural basis for the modulation of voltage-gated sodium channels by animal toxins. Science **362**, eaau2596 (2018).

13. Shen, H., Liu, D., Wu, K., Lei, J. & Yan, N. Structures of human $Na_v1.7$ channel in complex with auxiliary subunits and animal toxins. Science **363**, 1303–1308 (2019).
14. Hagen, N. A. *et al.* Tetrodotoxin for Moderate to Severe Cancer-Related Pain: A Multicentre, Randomized, Double-Blind, Placebo-Controlled, Parallel-Design Trial. *Pain research & management* 2017, 7212713 (2017).
15. Kishi, Y., Aratani, M., Fukuyama, T., Nakatsubo, F. & Goto, T. Synthetic studies on tetrodotoxin and related compounds. 3. A stereospecific synthesis of an equivalent of acetylated tetrodamine. J. Am. Chem. Soc. **94**, 9217–9219 (1972).
16. Kishi, Y. *et al.* Synthetic studies on tetrodotoxin and related compounds. IV. Stereospecific total syntheses of *DL*-tetrodotoxin. J. Am. Chem. Soc. **94**, 9219–9221 (1972).
17. Nishikawa, T., Urabe, D. & Isobe, M. An efficient total synthesis of optically active tetrodotoxin. Angew. Chem., Int. Ed. **43**, 4782–4785 (2004).
18. Hinman, A. & Du Bois, J. A stereoselective synthesis of (–)-tetrodotoxin. J. Am. Chem. Soc. **125**, 11510–11511 (2003).
19. Sato, K.-i. *et al.* Novel and Stereocontrolled Synthesis of (±)-Tetrodotoxin from myo-Inositol. J. Org. Chem. **70**, 7496–7504 (2005).
20. Sato, K.-i. *et al.* Stereoselective and efficient total synthesis of optically active tetrodotoxin from D-glucose. J. Org. Chem. **73**, 1234–1242 (2008).
21. Akai, S. *et al.* Total Synthesis of (–)-Tetrodotoxin from *D*-Glucose: A New Route to Multi-Functionalized Cyclitol Employing the Ferrier(II) Reaction toward (–)-Tetrodotoxin. Bulletin of the Chemical Society of Japan **83**, 279–287 (2010).
22. Maehara, T., Motoyama, K., Toma, T., Yokoshima, S. & Fukuyama, T. Total Synthesis of (–)-Tetrodotoxin and 11-norTTX-6(*R*)-ol. Angew. Chem. Int. Ed. **56**, 1549–1552 (2017).
23. Murakami, K., Toma, T., Fukuyama, T. & Yokoshima, S. Total Synthesis of Tetrodotoxin. Angew. Chem. Int. Ed. **59**, 6253–6257 (2020).
24. P. N. Marin (Esteve Pharmaceuticals SA), EP1785427A1. (2007).
25. Konrad, D. B. *et al.* A concise synthesis of tetrodotoxin. Science **377**, 411–415 (2022).
26. Keana, J. F. W., Mason, F. P. & Bland, J. S. Synthetic intermediates potentially useful for the synthesis of tetrodotoxin and derivatives. J. Org. Chem. **34**, 3705–3707 (1969).
27. Keana, J. F. W. & Kim, C. U. Synthetic intermediates potentially useful for the synthesis of tetrodotoxin and derivatives. II. Reaction of diazomethane with some shikimic acid derivatives. J. Org. Chem. **35**, 1093–1096 (1970).
28. Keana, J. F. W. & Kim, C. U. Synthetic intermediates potentially useful for the synthesis of tetrodotoxin and derivatives. III. Synthesis of a key lactone intermediate from shikimic acid. J. Org. Chem. **36**, 118–127 (1971).
29. Burgey, C. S., Vollerthun, R. & Fraser-Reid, B. Armed/Disarmed Effects and Adamantyl Expansion of Some Caged Tricyclic Acetals en Route to Tetrodotoxin1,2. J. Org. Chem. **61**, 1609–1618 (1996).

30. Noya, B. & Alonso, R. Radical cyclisation onto C-3 of 1, 6-anhydro-β-d-mannopyranose derivatives. Application to the formation of the C8a centre of (−)-tetrodotoxin. Tetrahedron Letters **38**, 2745–2748 (1997).
31. Noya, B., Paredes, M. D., Ozores, L. & Alonso, R. 5-exo Radical Cyclization onto 3-Alkoxyketimino-1,6-anhydromannopyranoses. Efficient Preparation of Synthetic Intermediates for (−)-Tetrodotoxin. J. Org. Chem. **65**, 5960–5968 (2000).
32. Cagide-Fagín, F. & Alonso, R. A cascade annulation based convergent approach to racemic tetrodotoxin. Eur. J. Org. Chem. **35**, 6741–6747 (2010).
33. Lago-Santomé, H., Meana-Pañeda, R. & Alonso, R. A Convergent Approach to the Dioxaadamantane Core of (±)-Tetrodotoxin. J. Org. Chem. **79**, 4300–4305 (2014).
34. Taber, D. F. & Storck, P. H. Synthesis of (−)-Tetrodotoxin: Preparation of an Advanced Cyclohexenone Intermediate. J. Org. Chem. **68**, 7768–7771 (2003).
35. Manabe, A., Ohfune, Y. & Shinada, T. Toward the total synthesis of tetrodotoxin: stereoselective construction of the 7-oxanorbornane intermediate. Tetrahedron Letters **55**, 6077–6080 (2014).
36. Mendelsohn, B. A. & Ciufolini, M. A. Approach to tetrodotoxin via the oxidative amidation of a phenol. Org. Lett. **11**, 4736–4739 (2009).
37. Chau, J., Xu, S. & Ciufolini, M. A. Assembly of a Key Dienic Intermediate for Tetrodotoxin via a Machetti–DeSarlo Reaction. J. Org. Chem. **78**, 11901–11910 (2013).
38. Baidilov, D. *et al.* Chemoenzymatic synthesis of advanced intermediates for formal total syntheses of tetrodotoxin. Angew. Chem., Int. Ed. **130**, 11160–11164 (2018).
39. Adachi, M. *et al.* Total Syntheses and Determination of Absolute Configurations of Cep-212 and Cep-210, Predicted Biosynthetic Intermediates of Tetrodotoxin Isolated from Toxic Newt. Org. Lett. **21**, 780–784 (2019).
40. Miyasaka, T., Adachi, M. & Nishikawa, T. Synthesis of the 8-Deoxy Analogue of 4,9-Anhydro-10-hemiketal-5-deoxy-tetrodotoxin, a Proposed Biosynthetic Precursor of Tetrodotoxin. Org. Lett. **23**, 9232–9236 (2021).
41. Nishikawa, K. *et al.* Tetrodotoxin Framework Construction from Linear Substrates Utilizing a $Hg(OTf)_2$-Catalyzed Cycloisomerization Reaction: Synthesis of the Unnatural Analogue 11-nor-6,7,8-Trideoxytetrodotoxin. Org. Lett. **23**, 1703–1708 (2021).
42. Nishiumi, M., Miyasaka, T., Adachi, M. & Nishikawa, T. Total Syntheses of the Proposed Biosynthetic Intermediates of Tetrodotoxin Tb-210B, Tb-226, Tb-242C, and Tb-258. J. Org. Chem. **87**, 9023–9033 (2022).
43. Good, S. N., Sharpe, R. J. & Johnson, J. S. Highly Functionalized Tricyclic Oxazinanones via Pairwise Oxidative Dearomatization and N-Hydroxycarbamate Dehydrogenation: Molecular Diversity Inspired by Tetrodotoxin. J. Am. Chem. Soc. **139**, 12422–12425 (2017).
44. Robins, J. G. & Johnson, J. S. An Oxidative Dearomatization Approach to Tetrodotoxin via a Masked ortho-Benzoquinone. Org. Lett. **24**, 559–563 (2022).

45. Cho, Y. S., Carcache, D. A., Tian, Y., Li, Y.-M. & Danishefsky, S. J. Total Synthesis of (±)-Jiadifenin, a Non-peptidyl Neurotrophic Modulator. J. Am. Chem. Soc. **126**, 14358–14359 (2004).
46. Xu, J., Trzoss, L., Chang, W. K. & Theodorakis, E. A. Enantioselective Total Synthesis of (–)-Jiadifenolide. Angew. Chem., Int. Ed. **50**, 3672–3676 (2011).
47. Yang, Y., Fu, X., Chen, J. & Zhai, H. Total Synthesis of (–)-Jiadifenin. Angew. Chem., Int. Ed. **51**, 9825–9828 (2012).
48. Yuan, C., Jin, Y., Wilde, N. C. & Baran, P. S. Short, Enantioselective Total Synthesis of Highly Oxidized Taxanes. Angew. Chem., Int. Ed. **55**, 8280–8284 (2016).
49. Ohtawa, M. *et al.* Synthesis of (–)-11-O-Debenzoyltashironin: Neurotrophic Sesquiterpenes Cause Hyperexcitation. J. Am. Chem. Soc. **139**, 9637–9644 (2017).
50. Condakes, M. L., Hung, K., Harwood, S. J. & Maimone, T. J. Total Syntheses of (–)-Majucin and (–)-Jiadifenoxolane A, Complex Majucin-Type Illicium Sesquiterpenes. J. Am. Chem. Soc. **139**, 17783–17786 (2017).
51. Leung, J. C. *et al.* Total Synthesis of (±)-Phomoidride† D. Angew. Chem., Int. Ed. **57**, 1991–1994 (2018).
52. Tomanik, M., Xu, Z. & Herzon, S. B. Enantioselective Synthesis of Euonyminol. J. Am. Chem. Soc. **143**, 699–704 (2021).
53. Wang, Y., Nagai, T., Watanabe, I., Hagiwara, K. & Inoue, M. Total Synthesis of Euonymine and Euonyminol Octaacetate. J. Am. Chem. Soc. **143**, 21037–21047 (2021).
54. Köbrich, G. & Werner, W. α-Chlorepoxyde, α-chloraldehyde und α-hydroxyaldehyde aus carbonylverbindungen und dichlormethyllithium. *Tetrahedron Lett.* **10**, 2181–2183 (1969).
55. Ken-ichi, S., Yasuhiro, K., Yutaka, N. & Juji, Y. Synthesis of the functionalized cyclohexanecarbaldehyde derivative. A potential key compound for total synthesis of optically active tetrodotoxin. Chemistry Letters **20**, 1559–1562 (1991).
56. Theurillat-Moritz, V. & Vogel, P. T.-a. Synthesis of enantiomerically pure 7-oxabicyclo[2.2.1]hept-2-enes precursors in the preparation of taxol analogues. Tetrahedron: Asymmetry **7**, 3163–3168 (1996).
57. Guidi, A., Theurillat-Moritz, V. & Vogel, P. Enantiomerically pure Diels-Alder adducts of maleic anhydride to furfural acetals through thermodynamic control. Single crystal and molecular structure of (1*S*, 4*R*, 4'*S*, 5'*S*)-1-(4', 5'-dimethyldioxolan-2'-yl)-5, 6-dimethylidene-7-oxabicyclo [2.2. 1] hept-2-ene. Tetrahedron: Asymmetry **7**, 3153–3162 (1996).
58. Chen, Y., McDaid, P. & Deng, L. Asymmetric alcoholysis of cyclic anhydrides. Chem. Rev. **103**, 2965–2984 (2003).
59. VanRheenen, V., Kelly, R. C. & Cha, D. Y. An improved catalytic OsO_4 oxidation of olefins to *cis*-1,2-glycols using tertiary amine oxides as the oxidant. Tetrahedron Lett. **17**, 1973–1976 (1976).
60. Crich, D. & Quintero, L. Radical chemistry associated with the thiocarbonyl group. Chem. Rev. **89**, 1413–1432 (1989).

61. Saraiva, M. F., Couri, M. R. C., Le Hyaric, M. & de Almeida, M. V. The Barton ester free-radical reaction: a brief review of applications. Tetrahedron **65**, 3563–3572 (2009).
62. Song, H.-T. *et al.* Photocatalytic decarboxylative hydroxylation of carboxylic acids driven by visible light and using molecular oxygen. Org. Lett. **81**, 7250–7255 (2016).
63. Zheng, C. *et al.* Ru-Photoredox-Catalyzed Decarboxylative Oxygenation of Aliphatic Carboxylic Acids through N-(acyloxy)phthalimide. Org. Lett. **20**, 4824–4827 (2018).
64. CronjéGrové, J., Holzapfel, C. W. & Williams, D. B. G. Stereoselective SmI_2-mediated conversion of carbohydrates into cyclopentanols. Tetrahedron Letters **37**, 1305–1308 (1996).
65. Chiara, J. L., Martínez, S. & Bernabé, M. Cascade Reaction of 6-Deoxy-6-iodohexopyranosides Promoted by Samarium Diiodide: A New Ring Contraction of Carbohydrate Derivatives. J. Org. Chem. **61**, 6488–6489 (1996).
66. Szostak, M., Spain, M. & Procter, D. J. Electron transfer reduction of unactivated esters using SmI_2–H_2O. Chem. Commun. **47**, 10254–10256 (2011).
67. Kim, K. S. & Qian, L. Improved method for the preparation of guanidines. Tetrahedron Lett. **34**, 7677–7680 (1993).
68. Feng, J., Kasun, Z. A. & Krische, M. J. Enantioselective Alcohol C–H Functionalization for Polyketide Construction: Unlocking Redox-Economy and Site-Selectivity for Ideal Chemical Synthesis. J. Am. Chem. Soc. **138**, 5467–5478 (2016).
69. Qiu, F. Strategic efficiency — The new thrust for synthetic organic chemists. Can J. Chem. **86**, 903–906 (2008).
70. Chen, T. G. *et al.* Building C(sp_3)-rich complexity by combining cycloaddition and C–C cross-coupling reactions. Nature **560**, 350–354 (2018).

Declarations

Acknowledgments

This work was supported by the National Natural Science Foundation of China (21971018 and 82225041). The authors gratefully acknowledge the Beijing Municipal Government and Tsinghua University for their financial support. We thank Prof. Joseph Ready and Prof. Uttam Tambar for their scientific comments and thank Drs. Jianwei Bian, Bo Liu, Shuanhu Gao, and Weiqing Xie for crucial suggestions.

Author contributions

X.Q. conceived the study; P.C., J.W., and X.Q. designed the synthetic route and prepared the manuscript; P.C. and J.W. carried out most of the chemical synthesis and prepared the supplemental information; P.C., J.W., Y.W., Y.S., and Q.W. analyzed the data; S.Z., X.C., and P.C. performed the biological study. All authors discussed the results and commented on the manuscript.

Competing interest declaration

The authors (Peihao Chen, Jing Wang, Yan Wang, Yuze Sun, Qingcui Wu, Xiangbing Qi) declare a patent application based on this study (WIPO Application No. PCT/CN2022/111861).

Additional information

Reprints and permissions information is available at http://www.nature.com/ reprints.

Correspondence and requests for materials should be addressed to Xiangbing Qi.

Publisher's note Springer Nature remains neutral with regard to jurisdictional claims in published maps and institutional affiliations.

Figures

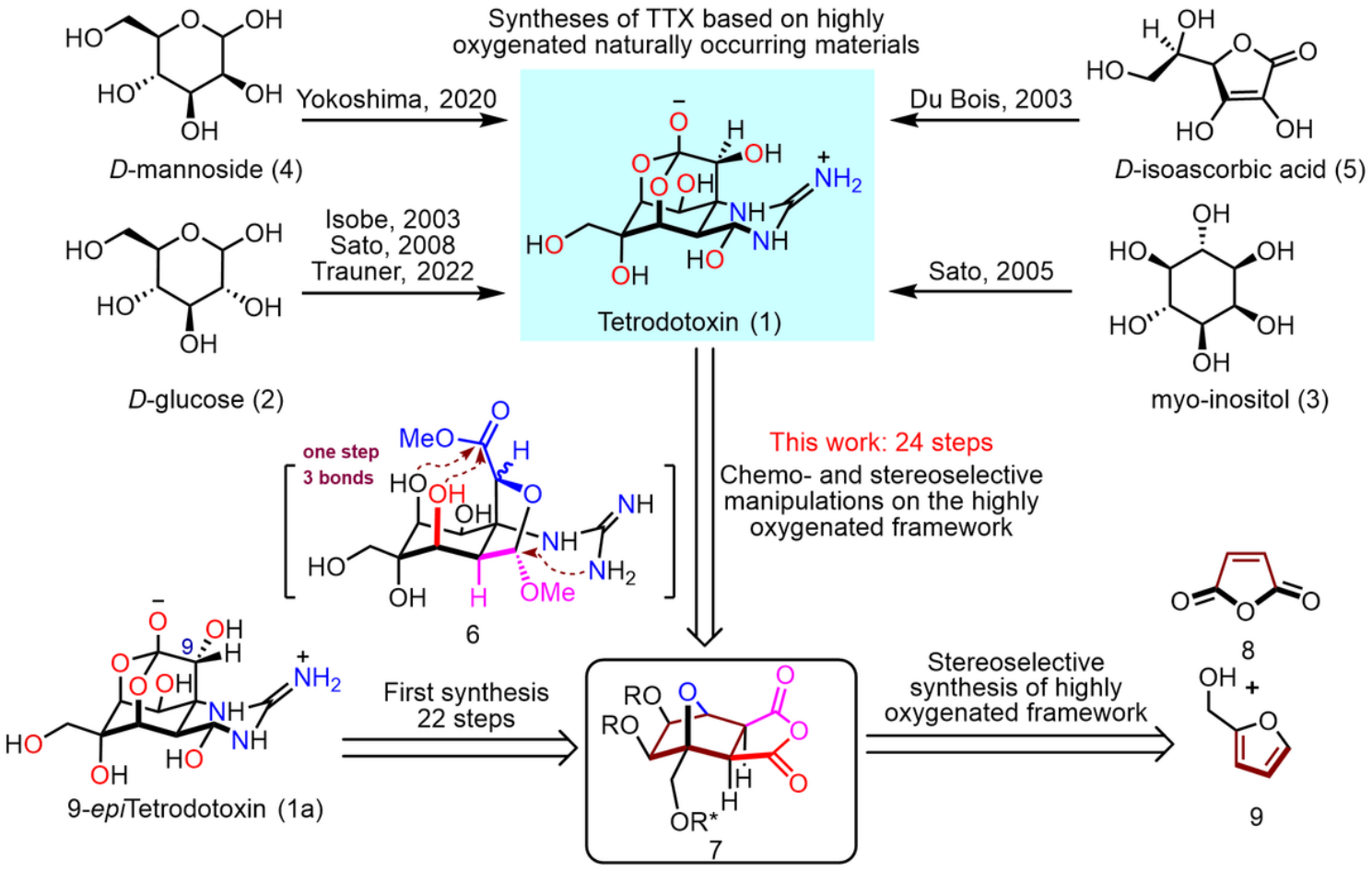

Figure 1

Previous syntheses of Tetrodotoxin and retrosynthetic analysis.

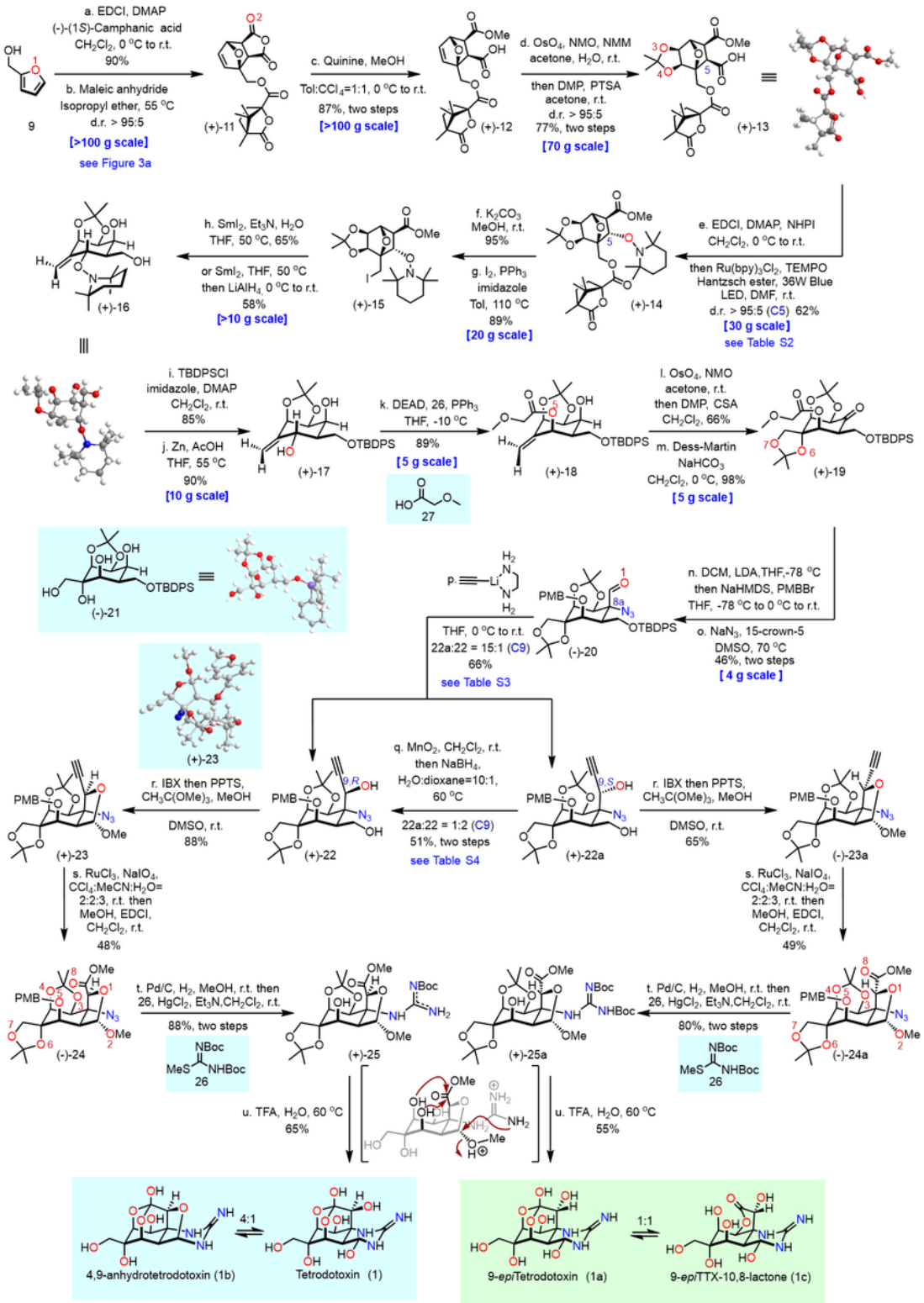

Figure 2

Completion of total synthesis of TTX and 9-*epi*TTX.

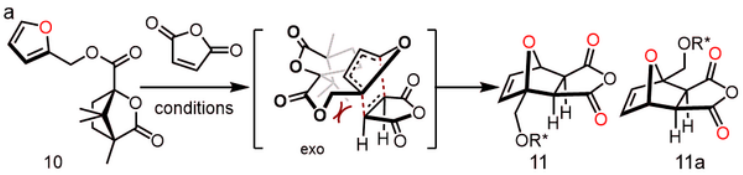

Entry	Maleic anhydride(eq.)	Solvent/Time(h)	(+)-11[%]	11:11a
1	1	Neat/24	36	5:4
2	1	Toluene/24	17	1:1
3	1	CH_3CN/24	17	5:6
4	1	Isopropyl Ether/24	66	1:10
5	1x2[a]	Isopropyl Ether/48	91[b]	>20:1

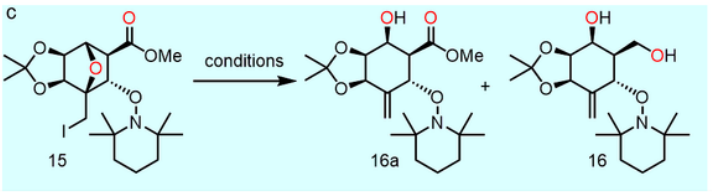

Entry	SmI_2 (equiv)	Additives	16a [%]	16 [%]
1	8	HMPA[a]	88	-
2	12	Et_3N/H_2O[b]	<5	77
3	12	Et_3N/H_2O[c]	<5	55
4	20	pyrrolidine/H_2O[d]	20	18
5	3	-	-	58[e]

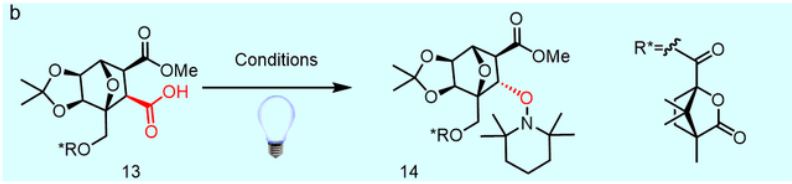

Entry	Conditions	Yield [%]	d.r.
1	Mes-AcrClO$_4$/ K_2HPO_4/ O_2/ blue LEDs then $NaBH_4$	<5	-
2	EDCI/ DMAP/1-Hydroxy-pyridinethione then ^{t}BuSH/ O_2/ Hg lamp then $P(OEt_3)$	<5	-
3	EDCI/ DMAP/ NHPI/ then $Ru(bpy)_3Cl_2$/ TEMPO/ Hantzsch ester/ blue LEDs	62[a]	> 95:5
4	EDCI/ DMAP/ NHPI then $Ru(bpy)_3Cl_2$/ TEMPO/ Hantzsch ester/ blue LEDs	66[b]	> 95:5

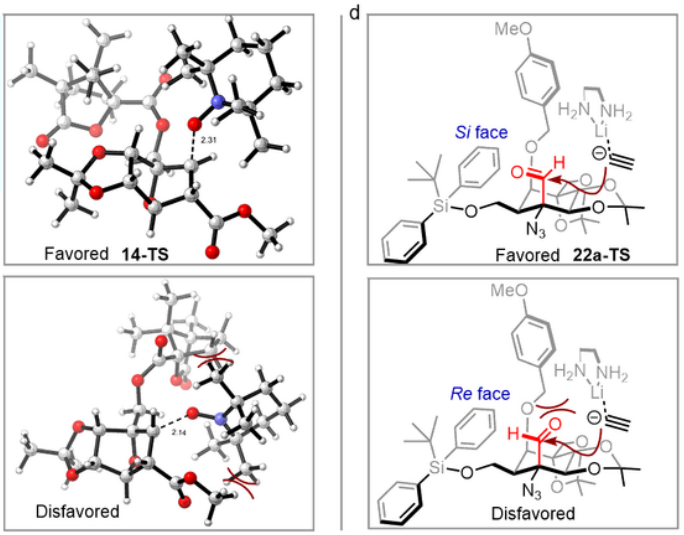

Figure 3

Optimization of reaction conditions. The yields were determined by ^{1}H NMR with 1,3,5-trimethoxybenzene as the internal standard. **a**, Optimization of the Diels-Alder reaction. [a] After 12h, the same eq maleic anhydride was added. [b] Scale up to 100 grams, isolated yield with 6% (molar ratio) maleic anhydride. **b**, Optimization of decarboxylative hydroxylation. [a] d.r. > 95:5, 30 g scale. [b] Isolated yield on 1 g scale using a circulating flow system, 24h. **c**, Optimization of the SmI_2/H_2O/amine-mediated fragmentation. [a] HMPA (10 eq). [b] Et_3N (24 eq)/H_2O (24 eq). [c] Et_3N (36 eq)/H_2O (36 eq). [d] pyrrolidine (60 eq)/H_2O (60 eq). [e] SmI_2 (3 eq), 55 ^{o}C, without purification followed by reduction using $LiAlH_4$. Isolated yields for the two steps on decagram scale. **d**, Selectivity of nucleophilic addition. *N.D., not determined. *NHPI: N-Hydroxyphthalimide, *MTBE: methyl tert-butyl ether.

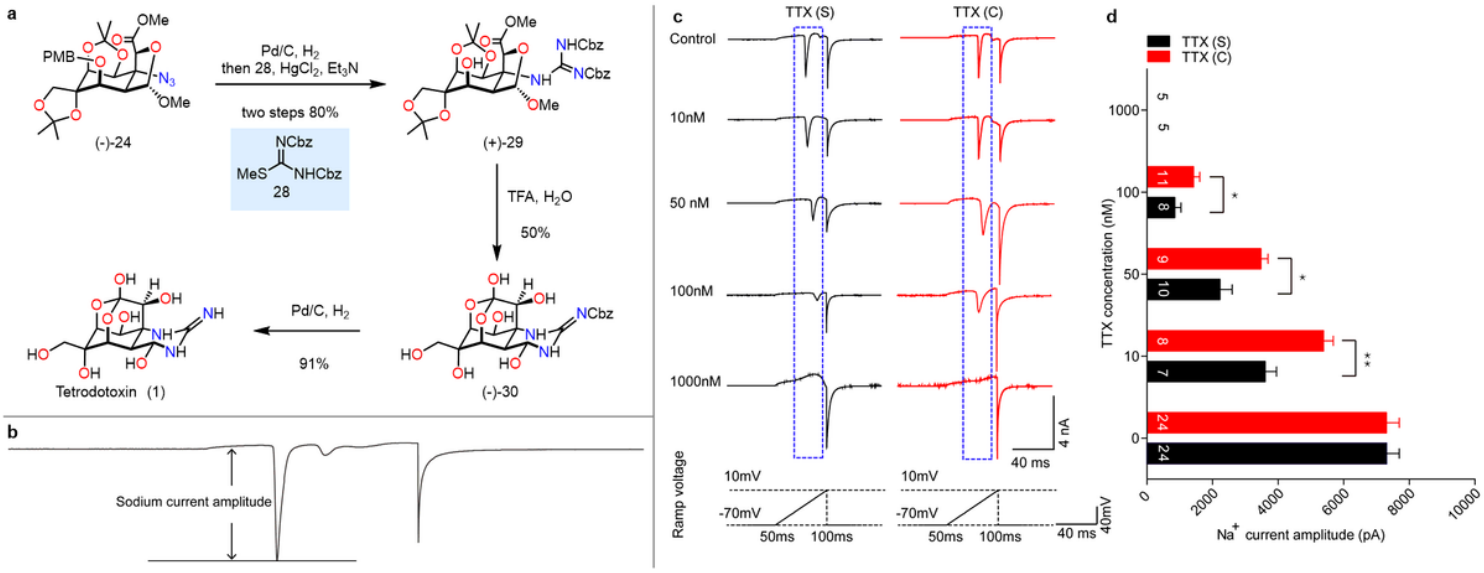

Figure 4

Alternative synthesis of pure TTX and effects of TTX (Synthetic) and TTX (Commercial) on depolarization-induced sodium currents. a, The procedure of preparing high purity TTX. **b**, Schematic diagram for sodium current evoked by a ramp voltage. **c**, Representative traces for sodium current amplitudes in primary cultured hippocampal neurons (DIV14) after treatment with various TTX compounds. Black, TTX (Synthetic); Red, TTX (Commercial). Ramp voltage from -70 mV to 10 mV over 50-ms. **d**, Quantitative analyses of sodium current amplitude in neurons treated with TTX (Synthetic) and TTX (Commercial) with various concentrations. Cell numbers are marked on the columns. Error bars represent means ±SEM; two-tailed unpaired t-test, *P < 0.05, **P < 0.01.

Supplementary Files

This is a list of supplementary files associated with this preprint. Click to download.

- Supplementaryinformation.pdf
- checkcifCCDC2182018.pdf
- CCDC2182018.cif
- checkcifCCDC2184298.pdf
- CCDC2184298.cif
- checkcifCCDC2184304.pdf
- CCDC2184304.cif
- checkcifCCDC2184305.pdf
- CCDC2184305.cif